

Modelization of resistive heating of carbon nanotubes during field emission

P. Vincent, S. T. Purcell,* C. Journet, and Vu Thien Binh

Laboratoire d'Émission Électronique, DPM UMR CNRS 5586, Université Lyon-1, Villeurbanne 69622, France

(Received 26 February 2002; published 6 August 2002)

In this paper we simulate the resistive heating of carbon nanotubes (CNT's) during field emission (FE) using the one-dimensional heat equation including radiation and conductive losses. The simulations are in relatively good agreement with our recent experiments in which we measured the heating of individual CNT's to as high as 2000 K during FE for currents I_{FE} of $\approx 2 \mu\text{A}$. For low temperatures where radiation is negligible the simulations reduce to an analytic solution that provides a universal guide to estimating current-induced heating in CNT's. The effects of this heating are included in the calculations of I_{FE} as a function of voltage.

DOI: 10.1103/PhysRevB.66.075406

PACS number(s): 73.63.-b, 79.70.+q, 61.46.+w

I. INTRODUCTION

One of the foremost proposed functions for carbon nanotubes (CNT's) is to serve as nanometric current carrying wires in nanoscience and nanotechnology and as a result there is now a large body of work on their electrical conductivity.^{1,2} Another important and related function is that they can be used as tips for field-emission sources,^{3,4} acting again as current carrying conductors. In both cases it is essential to understand the behavior of CNT's for high current densities and, in particular, their Joule heating as this will define important limits for applications. Despite the importance of the problem and its apparent tractability we have found no study in the literature on the modelization of the current-induced heating of CNT's.

This problem is all the more timely because recently Dean *et al.*⁵ and ourselves⁶ have shown by different methods the existence of heating of CNT's to very high temperatures during field emission (FE) for currents in the microampere range. In our case, the temperatures at the apex, T_A , of a clean nanotube were quantitatively determined from 300 K to 2000 K.⁶ This was done by field electron emission spectroscopy (FEES), in which the total energy distributions (TED's) of emitted electrons are measured. Furthermore the voltage drop along the CNT, and hence also its resistance R , were measured directly by the position of the TED peak. We found R to be $\approx 1 \text{ M}\Omega$ for CNT length of $\sim 40 \mu\text{m}$. The high temperatures were accompanied by light emission and both were concluded to be due to Joule heating along the CNT.

In this paper we present numerical simulations that support these conclusions. They are based on the one-dimensional (1D) heat diffusion equation including heat conduction and radiation and depend on the CNT dimensions and resistance directly measured in the experiment. We also compare these simulations to analytic solutions, which then serve as a general guide for CNT heating. In the last part we study the effect of the heating on the current-voltage relationship $I_{FE}(V)$ by including the temperature dependence of field emission.

II. HEAT EQUATIONS

In this paper we treat the nanotube as a simple resistance which is justified for our chemical vapor deposition (CVD)

nanotubes because mesoscopic behavior such as ballistic transport that is apparently observable in high-quality CNT's produced by arc discharge, is completely masked by the high defect concentration in such tubes.^{7,8} To investigate stable Joule heating during the FE process we model the CNT as a one-dimensional object of length L in contact with a heat sink fixed at temperature $T = T_0$ at $x=0$ and include heat losses by radiation on the length and the cap of the CNT, that is for a nanotube in the vacuum. The appropriate time-independent heat equation is

$$\kappa A \frac{\partial^2 T}{\partial x^2} dx - 2\pi r dx \sigma (T^4 - T_0^4) + dR I^2 = 0, \quad (1)$$

where κ is the thermal conductivity, A is the cross section, r the exterior tube radius, σ is the Stefan-Boltzmann constant (we assume emissivity=1), T_0 is the ambient temperature, dR is the resistance of a length element dx , and I is the current. Our approach is to find the simplest approximations that contain the essential physics. In reality κ and R are temperature dependent and vary greatly between nanotubes fabricated by different techniques.^{2,9} Because the CNT will have a temperature gradient they also vary with position along the tube. The experiment⁶ measured the total resistance R which decreased by $\approx 70\%$ as T_A increased from 300 to 2000 K. For this simulation we use $dR = R dx/L$ with $R = R(300 \text{ K}) - \alpha T$. $R(300 \text{ K})$ and α are chosen to match the experiment. κ is the only parameter that was not measured in the experiment and constant values found in the literature for CNT's fabricated by the same method of chemical vapor deposition are used.¹⁰

Radiation and temperature dependences of R and κ can be neglected for low temperatures. Equation (1) then has a useful analytic solution,

$$T(x) = T_0 + \frac{RI^2}{\kappa A} x - \frac{RI^2}{2\kappa AL} x^2, \quad (2)$$

which gives

$$T(L) - T_0 \equiv \Delta T_A = \frac{RL}{2\kappa A} I^2 = \frac{\rho}{2\kappa} \left(\frac{LI}{A} \right)^2 = \frac{\rho}{2\kappa} \frac{L^2 I^2}{\pi^2 r^4}. \quad (3)$$

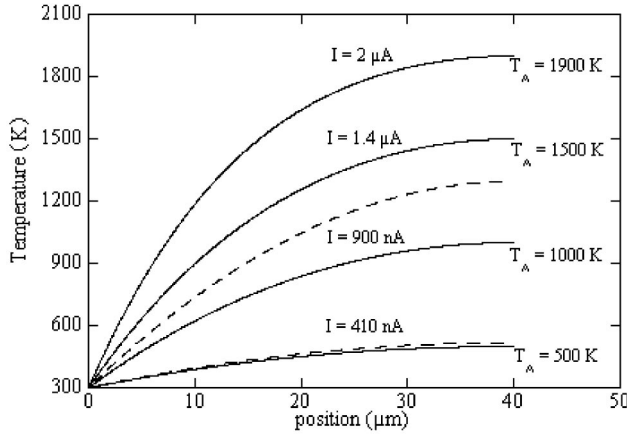


FIG. 1. Temperature profiles along a 40 μm length CNT for different currents simulated using Eqs. (1) (solid lines) and (2) (dashed lines). The parameters used for this simulation are indicated in Fig. 2.

The last form of Eq. (3) puts the accent on the intrinsic parameters and is found by substituting $R = \rho L/A$ with ρ the resistivity, $A = \pi r^2$ and neglecting the cross section of the inner tube hole which from TEM observations is $\sim 10\%$ of A for our multiwalled nanotubes (MWNT's). Equation (3) is useful for making quick estimates of the existence of appreciable heating in CNT's and shows how it scales with the different parameters, for example, it shows the strong inverse fourth power dependence on radius. In the important configuration of a CNT of length L' and resistance R' connected at both ends for electrical connections and direct conductivity measurements, the solution can be found from equation (3) by simply substituting $L = L'/2$ and $R = R'/2$. In this case the maximum temperature is at the center and not at the end. The formula emphasizes that though it is interesting to have long and thin nanotubes to reduce the voltages for FE this has, at constant κ and ρ , the counter effect of increasing the heating effects and reducing the maximum usable current.

III. SIMULATIONS AND COMPARISON WITH EXPERIMENTS

Simulations using Eqs. (1) and (2) for the temperature profiles along the CNT's for different I_{FE} and the CNT parameters of the experiment are shown in Fig. 1. They show that $\approx 50\%$ of the CNT is above $0.8\Delta T_A$ and that high values of T_A are reached at currents in the microampere range. The main result of this paper is shown in Fig. 2 where the simulated T_A versus I_{FE} is plotted (solid line) along with the experimental values for two different I/V cycles. The simulated T_A is in the same range as that of the experiment and thus the calculation supports the previous conclusion that the temperatures measured in the experiment were correct and due to Joule heating. In judging the agreement between simulation and experiment, the reader should bear in mind that in FE one typically measures current variations over six to eight orders of magnitude and these plots have a linear x axis in current. Thus an agreement better than an order of magnitude for these first-order calculations is already an achievement.

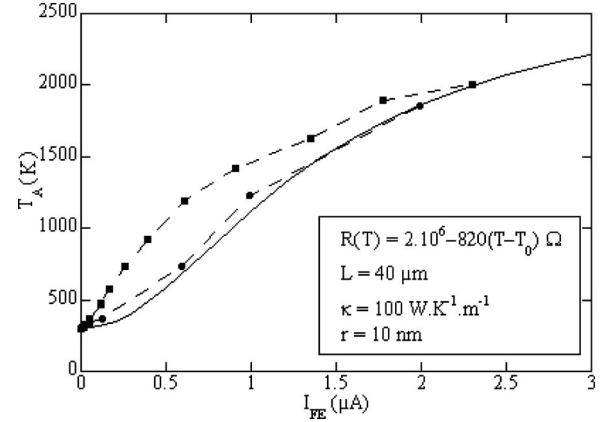


FIG. 2. Temperature at the apex of the nanotube, T_A , versus emission current I_{FE} using Eq. (1) (solid line). The data points are the experimental values for two runs (Ref. 6).

Plots using Eq. (2) are also shown in Fig. 1 for currents of 410 and 900 nA. As can be expected, the temperatures found neglecting radiation and the temperature decrease of R are higher and at low nanotube temperatures they approach those found allowing for radiation and $R(T)$. The deviation between the two is seen in Fig. 1 to be only 2% at 500 K but 30% at 1000 K. This means that Eq. (3) can be used rather well below 500 K for heating effects in the vacuum.

It is useful to turn Eq. (3) around to consider what is the minimum current I_{min} for which specific temperature rises occur. As two examples we estimate that the FEES method permits minimum temperature increases $\Delta T_{min} \approx 50$ K to be reliably distinguishable and that radiation effects are negligible below $\Delta T_A \approx 200$ K. In Table I we have calculated the value of I_{min} for $\Delta T_{min} = 50$ K using Eq. (3) for different MWNT's described in the literature, to show the large range

TABLE I. I_{min} for a temperature rise of 50 K calculated using Eq. (3) for different nanotubes described in the literature. The current is given for κ of 100 and 1000 $\text{W m}^{-1} \text{K}^{-1}$.

Reference	Length (μm)	Radius (nm)	Resistance (Ω)	I_{lim} (μA)
Fransen ^a <i>et al.</i> (Ref. 12)	3	22	10^5 ^b	7–22
	0.22	10	8×10^3 ^b	42–130
Ebbesen ^c <i>et al.</i> (Ref. 2)	3	3	9×10^4	1–3.2
	3	10.2	1×10^5	3.3–10
	3	6.3	1.5×10^9	0.02–0.05
	3	9.1	3×10^2	50–170
	3	5	10^8	0.05–0.16
	3	6.1	2.6×10^5	1.2–4
	3	7.4	3.6×10^4	4–12
Lee ^c <i>et al.</i> (Ref. 9)	4	50	10^5	14–45
Kaneto ^c <i>et al.</i> (Ref. 11)	20	20	2×10^5	1.8–5.6

^aFE experiment.

^bEstimated by the authors.

^c2 points or 4 points measures.

of I_{min} possible depending on the CNT parameters. We consider this analysis to be more valid for MWNT's than for single walled nanotubes (SWNT's) since thermal and electric conductivities can be more complicated in that case. We have selected only work where R , L , and r had been determined or at least estimated. The nonexhaustive data in Table I show I_{min} varying from 20 nA to 170 μ A.

IV. EFFECT OF TEMPERATURE ON I/V CHARACTERISTICS

FE current is an increasing function of temperature and therefore the current should increase above the Fowler-Nordheim (FN) line, which assumes constant temperature, at higher currents where heating occurs. This has been observed experimentally.^{5,6} The higher current then creates a positive feedback mechanism for still more increased current by creating additional heating. In this section we combine the FN law extended to include temperature effects with the heating simulations to calculate $I_{FE}(V)$ for fixed temperature at the base tip. Note that to measure temperatures we have used an energy analyzer which is not often installed in FE chambers. Thus in addition to providing added confirmation of the heating effects, the I/V curves potentially provide a simple alternative method for researchers to quantify the temperature rises.

The effect of temperature on FE current is given by¹³

$$I(V, T) = I_0(V) \frac{\pi p}{\sin(\pi p)} \approx I_0(V) \left[1 + \frac{1}{6} \left(\frac{\pi K_B T}{d} \right)^2 \right], \quad (4)$$

$I_0(V)$ is the FN law given by

$$I_0(V) = AF^2 \exp[-B\phi^{3/2}/\beta V]. \quad (5)$$

$p = K_B T/d$, $d \equiv F(V/\text{\AA})/\sqrt{\phi(\text{eV})}$, ϕ is the work function and F is the field given by $F = \beta V$ with V the applied voltage and β a constant for a system of fixed electrodes. A and B vary little with voltage and are taken as constants. The problem is now solved iteratively between Eqs. (1), (4), and (5) to give $I_{FE}(V)$.

In Fig. 3 we show simulated and experimental⁶ $I_{FE}(V)$ data plotted both conventionally against $1/V$ and against V . The small dashed line defined as I_F is found by fitting the portion of the experimental data below which heating effects occur to the FN law. The calculated and measured emitted currents are higher than those predicted using only Eq. (5). However on such a plot the experimental current increases are not so striking and could, in fact, be due to other effects such as field-induced apex sharpening or work function reduction. This is why the TED's were necessary to definitively prove the existence of temperature rises.

Simulations are shown assuming both R decreasing with temperature as above and also assuming R to be constant. In the latter case (dashed arrow) I_{FE} increases more abruptly with voltage which supports the hypothesis⁶ that the intrinsic negative resistance coefficient of the CNT's is important for allowing stable high temperatures induced by the FE current.

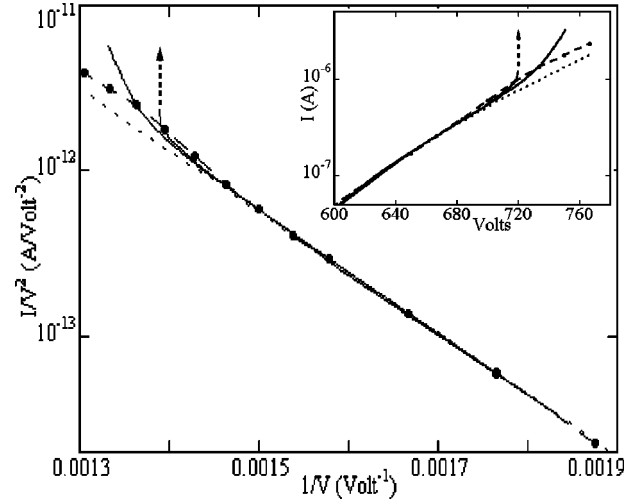


FIG. 3. Simulated and experimental Fowler-Nordheim plots obtained in the presence of heating effects. The dark points are the experimental data, the line of small dashes is the FN fit (see text), and the solid lines are the simulated curves. The dashed arrow indicates the current simulation in the case of constant R .

The temperature rise in the simulation and experiment occur for the same voltage and current range.

The heating effect is more visible if we plot $\Delta I/I_F$ defined in Fig. 4 versus V for both experiments and simulations. $\Delta I/I_F(V)$ rises abruptly with current at a specific voltage. The voltage is lower and the rise practically vertical for constant R . We see that the experimental $\Delta I/I_F$ also increases abruptly with V until the highest currents where the last two data points fall off the rising curve. These temperatures obviously cause a modification of the CNT. We have confirmed this behavior with numerous measurements at high currents. It occurs in the 1600–2000 K range and has been previously reported.⁵ Again to judge the quality of the agreement between experiment and theory, note that this is a linear plot of the difference of two currents that vary exponentially in voltage. The fact that the fast increase in current occurs in the same voltage range is a further confirmation of the validity of the temperature measurements.

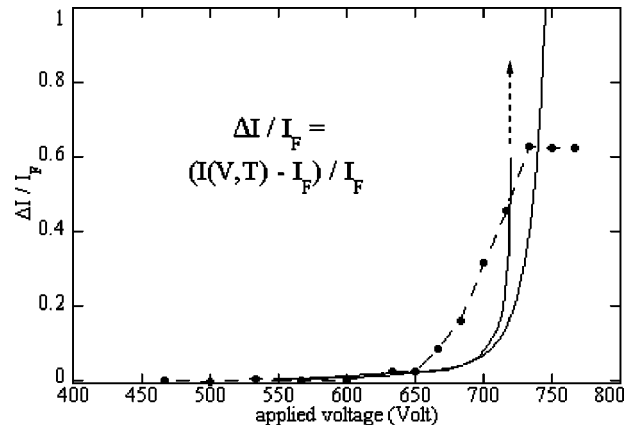


FIG. 4. $\Delta I/I_F$ versus applied voltage. Experimental data (dashed line) and numerical simulations (solid lines) are plotted in the case of R decreasing with T or constant (extended by the arrow).

V. DISCUSSION

An increase in the $I_{FE}(V)$ curve above the FN plot at high current has been previously measured by Dean *et al.*⁵ and ascribed to the temperature dependence of the FE current given by Eq. (4). However, the authors invoke a different heating mechanism. Based on our earlier work on nanotips,¹⁴ they have proposed that the high temperatures are due to a local heating at the nanotube end due to the Nottingham effect. Though we agree that this may be part of the problem, for example, as a mechanism for initial current-induced cleaning of nanotubes,¹⁵ there are several arguments against this being the major heating mechanism in our experiments. First, the large local heating effects referred to above depend on the existence of distinct peaks in the TED's well below E_F that shift linearly with the applied field and are due to the precise atomic structure of a nanotip at the emission site. Our TED's do not have the peak structure and yet we measure high stable temperatures. In fact, we have carried out some preliminary simulations that include the Nottingham effect using the measured TED's to find the average energy loss or gain and the emitted current. We find corrections to the calculated temperatures of the order of $\pm 10\%$ at 2000 K, depending on which series of TED is used. This is appreciable but still of second order. In general, the Nottingham effect is considerably diminished because the TED's tend towards a symmetric shape at the higher temperatures caused by Joule heating, which implies a relatively low average energy exchange per electron emitted. Second, the peak structures in the nanotip TED's are not reproducible and vary largely in form with the structure of the nanotip, as does the emission current. At high currents the nanotips undergo rapid changes in structure accompanied with wildly varying energy spectra and currents and often undergo sudden destruction. In our experiments the current and heating were stable effects. Third, local heating would generate a hot spot concentrated at the end of the nanotube which would not provide enough light to be visible by the naked eye as we have observed. Finally in this work we show that the experimental and simulated temperatures are consistent with resistive heating which must *a priori* be taken into account.

The modelization predicts temperature increases without limit as a function of increasing current. However, field assisted evaporation will set in at high temperatures to modify the nanotube and limit the temperature rises, as pointed out by Dean *et al.* Length reduction will occur, which reduces

the resistance and the field at the tip of the CNT and hence the heating and emitted currents. These effects can be seen in Fig. 4 where the last two experimental currents drop below the rising curve because of nanotube modification at high currents. We are currently studying this by simulation to quantify the induced nanotube modifications.

We have argued above that the heating controls the maximum current, I_{max} , that a nanotube can support. This is a technologically important parameter. Simulations using the heat equations must be carried out to estimate I_{max} accurately as no analytic formulas exist which describe how the combined effects of Joule heating, heat conduction and radiation depend on the specific nanotube parameters and their dependence on temperature. However, a simple order of magnitude estimate is suggested from our simulations and experiments. We note first that from experiments and Eq. (3), $I \sim 400$ nA for $T_A \sim 500$ K. Second, nanotube modification begins at $T_A \sim 1600-2000$ K for $I \sim 2$ μ A, i.e., an increase of five times in the current. Thus we propose an order of magnitude estimate is

$$I_{max} \sim 5I_{500K} \quad (6)$$

where I_{500K} is calculated for specific nanotube parameters from Eq. (3).

VI. CONCLUSION

These simulations demonstrate that a one-dimensional calculation for current-induced heating in carbon nanotubes is a necessary and fruitful first-order approach. It gives temperatures in the range of the experiment confirming that the heating during FE measured experimentally is due to a Joule effect. The key was that the experiment gave access to R , T , L , and r for semiquantitative comparisons. For better comparisons we will need to have better measurements of the dimensions of the CNT in question. The deviations between experiment and theory will then give us access to other fundamental processes such as the temperature dependence of R and κ , Nottingham heating effects and induced nanotube modifications. From the point of view of applications, this heating process has been shown to permit CNT cleaning without external temperature⁶ and to lead to the partial or complete destruction of CNT's, setting the maximum current one can extract from CNT's in FE devices. The simulations now provide a firm basis for analyzing and controlling these processes.

*Electronic address: purcell@dpm.univ-lyon1.fr

¹See, for example, C. Dekker, Phys. Today **52** (5), 22 (1999).

²T.W. Ebbesen, H.J. Lezec, H. Hiura, J.W. Bennett, H.F. Ghaemi, and T. Thio, Nature (London) **382**, 54 (1996).

³W. de Heer, A. Châtelain, and D. Ugarte, Science **270**, 1179 (1995).

⁴J.-M. Bonard, H. Kind, T. Stöckli, and Lars-Ola Nilsson, Solid-State Electron. **45**, 893 (2001).

⁵K.A. Dean, T.P. Burgin, and B.R. Chalamala, Appl. Phys. Lett. **79**, 1873 (2001).

⁶S.T. Purcell, P. Vincent, C. Journet, and Vu Thien Binh, Phys. Rev. Lett. **88**, 105502 (2002).

⁷S. Roche, F. Triozon, and A. Rubio, Appl. Phys. Lett. **79**, 3690 (2001).

⁸S. Roche, F. Triozon, A. Rubio, and D. Mayou, Phys. Rev. B **64**, 121401 (2001).

⁹S. -B. Lee, K. B. K. Teo, M. Chhowalla, D. G. Hasko, G. A. J. Amaratunga, W. I. Milne, and H. Ahmed, Microelectron. Eng. (to be published).

¹⁰W. Yi, L. Lu, D.L. Zhang, Z.W. Pan, and S.S. Xie, Phys. Rev. B **59**, R9015 (1999).

¹¹K. Kaneto, M. Tsuruta, G. Sakai, W.Y. Cho, and Y. Ando, Synth. Met. **103**, 2543 (1996).

- ¹²M.J. Fransen, T.L. van Rooy, and P. Kruit, *Appl. Surf. Sci.* **146**, 312 (1999).
- ¹³L.W. Swanson and A.E. Bell, *Adv. Electron. Electron Phys.* **32**, 193 (1973).
- ¹⁴V. T. Binh, N. Garcia, and S. T. Purcell, in *Advances in Imaging and Electron Physics*, edited by P. Hawkes (Academic, New York, 1996), Vol. 95.
- ¹⁵V. Semet, B. Vuthien, P. Vincent, D. Guillot, K. B. K. Teo, M. Chhowalla, G. A. J. Amaratunga, B. Milne, P. Legagneux, and D. Pribat, *Appl. Phys. Lett.* (to be published).